

ORIGINAL INNOVATION

Open Access



Advanced framework for post-flood assessment of steel truss bridges under data-constrained conditions: integrating engineering insights and empirical fragility models

Saman Mansouri^{1,2}, Ilaria Venanzi^{3*} , Filippo Ubertini³ and Chiara Biscarini¹

*Correspondence:
ilaria.venanzi@unipg.it

¹ WARREDOC - Water Resources Research and Documentation Center, Università per Stranieri di Perugia, Perugia, Italy

² FABRE Consortium, the Italian Research Consortium for the Evaluation and Monitoring of Bridges, Viaducts, and Other Structures, Perugia, Italy

³ Department of Civil and Environmental Engineering, University of Perugia, Perugia, Italy

Abstract

Bridges are vital components of a country's infrastructure, playing a crucial role in transportation networks. However, natural hazards such as floods significantly threaten their stability and serviceability. The increasing frequency and intensity of floods due to climate change have heightened concerns about the serviceability of bridges after the floods. Despite their critical importance and high risk of vulnerability to floods, limited research has examined the failure mechanisms and their contributing factors on steel truss bridges, as one of the most widely used types of bridges. This knowledge gap remains a major challenge in the field. Previous studies have primarily assessed bridge vulnerability to floods through qualitative analyses or finite element modeling, often overlooking the specific failure characteristics of collapsed bridges and their empirical fragility curves. Addressing this limitation, the present study investigates the catastrophic 2019 Poldokhtar flood (one of the most devastating floods in Iran in recent decades) and its impact on eight steel truss bridges. Through extensive field investigations and the development of empirical fragility curves, this research provides a detailed assessment of bridge performance during extreme flood events. The study identifies key failure mechanisms and damage scenarios based on visual inspections, engineering judgment, and empirical analyses. Furthermore, to overcome data scarcity and site-specific uncertainties, this study introduces a novel flood intensity measure relating floodwater height to bridge deck elevation. This practical indicator enables consistent comparison across different hydraulic conditions and serves as a valuable tool for evaluating bridge vulnerability under real-world flood scenarios.

Keywords: Structural performance, Poldokhtar flood, Steel truss bridge, Flood damage assessment, Empirical fragility curves

1 Introduction

Bridges are fundamental components of transportation networks (Guikema and Gardoni 2009), serving as critical links that facilitate the movement of goods and people. Beyond their role in daily transportation, they play a crucial role during emergencies and natural disasters (Mitoulis et al. 2022; Rezvani et al. 2024). The increasing demand for bridge construction is driven by factors such as urban expansion, critical infrastructure needs, road and rail network development, traffic mitigation, economic growth, and disaster resilience (Mansouri 2020, Mansouri and Noroozinejad Farsangi 2024). Consequently, resilient bridge construction has become a key requirement for modern infrastructure development, addressing both present and future societal demands (Mansouri et al. 2022; Wang et al. 2023; Allen et al. 2023).

Despite significant advancements in engineering and technology that have enhanced the resilience of structures, many existing bridges remain vulnerable to natural disasters such as floods and earthquakes (Mansouri 2021; Yilmaz and Banerjee 2018). This underscores the need for continuous innovation in bridge design, retrofitting, and assessment methodologies to mitigate potential risks effectively (Kosic et al. 2023; Karriqi et al. 2024).

Climate change has intensified the frequency and severity of floods, posing a growing threat to bridge infrastructure. Floods rank among the most destructive natural disasters affecting bridges. For instance, Lamb et al. (2019) reported that between 1846 and 2012, over 100 bridges on the UK railway network suffered severe flood damage. Similarly, in 2015, floods damaged 235 roads and footbridges in Cumbria. In Iran, Mansouri and Pouraminian (2022) documented the destruction of more than 15 bridges in Lorestan province due to flooding in 2020. Additionally, Lee et al. (2013) conducted a statistical study analyzing 1,254 bridge failures from 1980 to 2012, further emphasizing the vulnerability of these structures to flood hazards. This challenge expresses the urgent need to adapt infrastructure and disaster preparedness strategies to mitigate the impacts of climate change-induced flooding (Burghardt et al. 2025; Pucci et al. 2023). The occurrence of flood-induced bridge collapses in recent years emphasizes the imperative of systematically assessing structural performance under extreme flood scenarios.

Numerous studies have investigated the impact of floods on human life, economic losses, and structural damage. Notable contributions include those by Pistrika and Tsakiris (2007), and Jonkman et al. (2008). Kerenyi (2009) examined hydrodynamic forces on bridge decks. Researchers such as Scawthorn et al. (2006a, 2006b) and Torres et al. (2014) proposed general methodologies for assessing flood hazards. Drdácáký (2010) explored flood damage to historic structures, whereas Chung and Adeyeye (2018) evaluated flood-induced structural damage.

Ataei and Padgett (2013) performed numerical sensitivity analyses on key factors influencing bridge vulnerability, including fluid–structure interaction effects. Kim et al. (2017) introduced an innovative method for developing flood fragility curves for bridges. Wang et al. (2019) investigated the impact of bridge columns during floods.

Debris impact and debris damming are critical factors contributing to bridge failures during floods. These processes cause water accumulation on the upstream side of the bridge, exerting additional pressure on the structure, as discussed by Xia et al. (2018),

Okamoto et al. (2020), Panici and Almeida (2020), Cicco et al. (2020), and Hasanpour et al. (2022).

Marvi (2020) reviewed analytical methods for assessing flood damage to structures. Xiao et al. (2021) investigated the effects of floods on masonry structures. In a study, Mitoulis et al. (2021) conducted the first international assessment of restoration models to quantify bridge flood resilience, developing reliable recovery models. Argyroudou and Mitoulis (2021) highlighted the limitations of earlier studies, which primarily relied on qualitative analyses and visual inspections. Their work introduced advanced fragility models that accounted for complex interactions between water, soil, and bridge structures, revealing that integral bridges are more susceptible to local scour than those with bearings due to their reduced flexibility.

Various classifications have been proposed for flood-induced structural damage states. For example, Padgett et al. (2012) used the HAZUS framework and defined four damage states (slight, moderate, extensive, and complete). More recently, Pucci et al. (2023) introduced a four-level categorization, which considers undamaged, slightly damaged, moderately damaged, and extensively damaged conditions.

Greco and Lonetti (2022) examined the vulnerability of coastal and inland bridges to flooding. Additionally, Paulik et al. (2022) reviewed flood risk assessment methodologies for residential buildings, while Kelesoglu et al. (2023) evaluated structural flood damage in the Western Black Sea Basin, where 76 fatalities were reported, and over 30,000 people were affected. Habeeb and Bastidas-Arteaga (2023) examined the impact of climate change on the stability of river-crossing bridges. Their study employed hydrological modeling, flood frequency analysis, and a stochastic Poisson process to assess the probability of exceeding design flood levels under various climate scenarios. Han et al. (2023) numerically analyzed the collapse mechanism of the Putang Bridge, a historical multi-span stone arch bridge, under flood-induced forces. Utilizing computational fluid dynamics simulations and finite element modeling, they investigated hydrodynamic pressure, drag, and lift forces at different flood levels, providing valuable insights into bridge vulnerability and potential mitigation strategies.

Barbera et al. (2024) characterized building damage caused by floods in Spain. Komolafe et al. (2024) explored flood damage models and influencing factors in a data-scarce river basin. Mansouri et al. (2024, 2025) conducted studies on structures damaged by flooding, contributing to the understanding of structural failures under extreme floods. Xiaofei et al. (2024) investigated the collapse mechanisms of masonry arch bridges during floods using numerical and stochastic analyses. Their study of the 2020 Zhenhai Bridge collapse revealed that the combined effects of scour and water flow played a significant role in structural failure. They emphasized the importance of stochastic analysis in assessing bridge safety under extreme flood conditions. Burghardt et al. (2025) examined bridge damage during the 2021 Western Europe floods, particularly in Germany. Their statistical analysis revealed that bridge height, proximity to residential areas, and debris accumulation had a significant influence on the severity of structural failures.

However, one of the most critical challenges in flood risk assessment is the scarcity of reliable data. In many regions, hydrological and hydraulic records are incomplete, the structural details of existing bridges are poorly documented, and real-time monitoring systems are absent. Following severe flood events, post-disaster investigations

often rely only on visual inspections and fragmented reports, which substantially limit the accuracy of vulnerability assessments. Conventional approaches, such as finite element modeling and large-scale hydraulic simulations, though powerful, require detailed datasets that are rarely available in post-flood contexts. This highlights the urgent need for practical and data-efficient frameworks that integrate engineering judgment, empirical evidence, and simplified yet robust indicators to examine the effects of floods on bridges. To address this gap, the present study focuses on steel truss bridges affected by the catastrophic 2019 Poldokhtar flood in Iran. Through extensive field investigations and the introduction of a novel flood intensity measure based on the relative elevation of floodwater and bridge deck, a systematic framework is established for evaluating bridge performance under data-constrained conditions. This approach not only enables the development of empirical fragility models but also provides a practical tool for enhancing flood resilience assessment in regions lacking comprehensive datasets. Given that previous numerical and experimental research has mainly focused on individual structures, a comprehensive field-based investigation and the development of empirical fragility curves grounded in real-world evidence are essential; this study addresses that need by establishing a robust database of flood-induced bridge damage and deriving empirical fragility functions.

2 Methodology

The objective of this study is to systematically assess steel truss bridges' damage under flood hazards through a step-by-step methodological framework (Fig. 1). First, extensive field investigations are conducted before, during, and after flood events to collect photographs and videos that provide a detailed visual record of bridge performance under extreme conditions. Complementary information about flood conditions and river characteristics is obtained from official reports. The data gathered from both field observations and documentary sources are systematically classified to create a coherent dataset. Based on engineering judgment and visual inspections, bridge damage is categorized

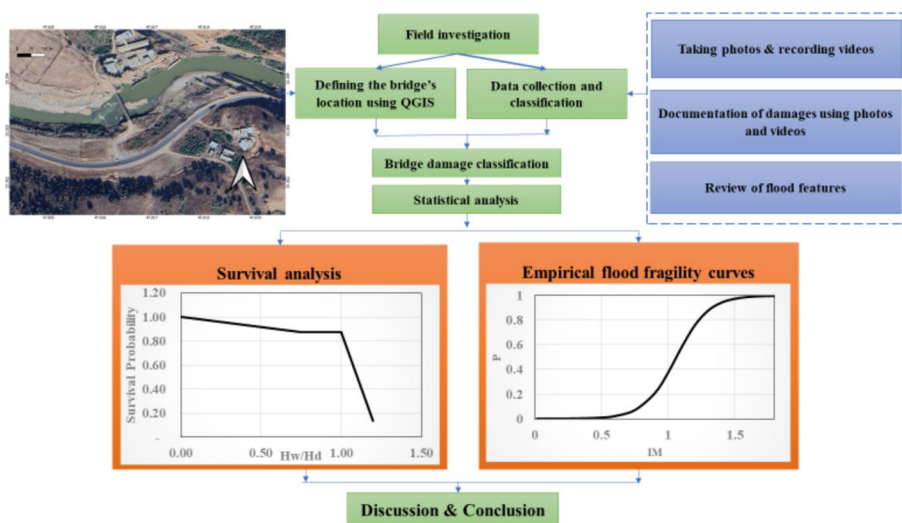


Fig. 1 Workflow of the proposed framework

into four levels: slight, moderate, extensive, and collapse. Table 1 summarizes the damage classification adopted in the present study, which is derived from a comprehensive combination of field observations, photographic and documentary evidence, and expert engineering judgment. Expert evaluations are further employed to identify the main causes of bridge damage, including pier scour, hydrodynamic pressure, and debris impact. Subsequently, a set of statistical assessments is performed. In particular, the Kaplan–Meier survival analysis method is employed to estimate the probability of bridge survival under different flood intensity levels. Additionally, an empirical flood fragility curve is developed using field data and expert judgment. Finally, the findings are synthesized and interpreted, leading to the development of empirical fragility models and the provision of practical recommendations for both designing flood-resilient bridges and retrofitting existing structures.

2.1 A novel flood intensity index

Post-flood assessment of bridges under data-scarce conditions remains a major challenge, as hydrological and structural information is often incomplete. Bridges are typically located along extended rivers with multiple tributaries, which exposes each structure to distinct flow discharges and velocities. Moreover, variations in topography and channel morphology result in different hydraulic capacities at the location of each bridge. Additionally, deck elevations vary significantly among bridges, resulting in floods interacting with each structure at various intensities. These factors lead to uncertainties and hinder realistic evaluations of bridge vulnerability. To address this limitation, the present study introduces a novel and practical parameter: the ratio of floodwater height to bridge deck elevation. This simple yet meaningful index enables consistent comparisons across diverse hydraulic conditions and provides an effective tool for assessing flood impacts on bridges in data-constrained environments. This study introduces a new parameter for flood intensity measure (IM), defined as the ratio of water height (Hw) to deck height (Hd). This parameter is used to classify three levels of flood-induced bridge damage. The flood is categorized into three risk levels based on the (Hw/Hd) ratio (Fig. 2 and Table 2). Figure 2 also illustrates the vital connections in bridges and the deck–abutment contact conditions with and without mechanical connections. Hazard levels I, II, and III correspond to $IM < 0.75$, $0.75 \leq IM < 1$, and $1 \leq IM$, respectively.

Table 1 Bridge damage level classification based on field evaluation

Damage levels	Description of damage
Slight (minor)	<ul style="list-style-type: none"> - The bridge remains consistently usable. - The bridge functions without interruption. - Concrete cover experiencing spalling
Moderate	<ul style="list-style-type: none"> - Several plastic hinges can be found on the bridge. - Retrofitting takes minimal time, and bridges can be repaired swiftly. - There is limited damage to piers, foundations, and bearings.
Extensive	<ul style="list-style-type: none"> - Numerous plastic hinges are present on bridges. - Significant time is needed to retrofit bridges. - Buckling occurs in the piers and deck. - Some elements exhibit deep cracks.
Collapse (complete)	<ul style="list-style-type: none"> - The bridge deck has been slid and overturned. - Columns, bearings, cap beams, and abutments are extensively damaged. - In this scenario, both the bridge and its structural elements collapse.

complexity of hydraulic loading, and future studies with more comprehensive datasets should extend this framework toward multi-parameter intensity measures.

2.2 Survival analysis method and its application in assessing bridge vulnerability

Survival analysis has been increasingly adopted in risk assessment and structural stability studies, owing to its ability to handle progressive deterioration and threshold-type responses without imposing restrictive distributional assumptions (e.g., Fang et al. 2018; Wettach-Glosser et al. 2020; Cartiaux et al. 2024). In this research, survival analysis is employed as a probabilistic framework to characterize the vulnerability of truss bridges subjected to flooding, with particular emphasis on the Kaplan–Meier estimator. This estimator is used as a nonparametric tool to derive the empirical survival function from observed bridge performance data. Within this context, flood severity is parameterized by the ratio H_w/H_d , which is interpreted as an equivalent time-like variable, while bridge performance is expressed in terms of the probability of remaining below predefined damage limit states over increasing levels of H_w/H_d . The survival function $S(H_w/H_d)$ is thus defined as the probability that a bridge remains intact (i.e., does not reach the specified damage state) up to a given value of H_w/H_d . In this study, “time” is defined as a parameter equivalent to flood severity (H_w/H_d); thus, the survival function represents the probability of bridges remaining intact up to a given H_w/H_d (Eq. 1). If d_i is the number of bridges that failed within a specific H_w/H_d range and n_i is the total number of bridges exposed to risk at that level, the survival function is computed as expressed in Eq. (1). Through this formulation, the evolution of bridge survival probability with increasing flood severity is quantified in a stepwise manner, providing clear insight into the mechanisms governing damage progression in truss bridges under flood conditions.

$$S(t) = \prod_{t_i \leq t} \left(1 - \frac{d_i}{n_i} \right) \quad (1)$$

where:

$S(t)$: estimated survival probability at time t .

t_i : a time point (or increasing level of hazard, e.g., flood severity) at which an event (e.g., failure) occurs

d_i : number of failures (e.g., collapsed bridges) at t_i

n_i : number of subjects (e.g., bridges at risk) just before t_i

\prod : Denotes the cumulative product over all event times $t_i \leq t$

2.3 Empirical fragility curve

In the present research, empirical fragility curves are employed as probabilistic tools to quantify the vulnerability of steel truss bridges exposed to the 2019 flood event in Pol-dokhtar. These curves express the probability that the structural response exceeds predefined damage limit states as a function of a newly defined flood intensity measure. The formulation is grounded in the principles of conditional probability, whereby, for each specified level of flood intensity, the likelihood of reaching or surpassing a given

damage state is estimated. Unlike analytical or numerical simulation-based approaches, the empirical framework adopted in this study relies directly on documented flood characteristics and observed post-event bridge damage. The primary objective of developing flood fragility curves (FCs) is to quantify the probability of bridge failure or exceedance of specific damage states under varying flood intensity levels. FCs provide a probabilistic linkage between flood hazard severity and observed structural performance, thereby enabling quantitative flood risk assessment and supporting informed decision-making for mitigation, emergency planning, and retrofit prioritization (Kim et al. 2017; De Risi et al. 2020; Ahamed et al. 2021; Arora and Banerjee 2023).

In this study, fragility curves are derived directly from post-flood field surveys and expert-based damage evaluations. Each bridge is classified into a discrete damage state according to the criteria summarized in Table 1, and the resulting empirical damage data are subsequently associated with the corresponding flood intensity index, defined as the ratio H_w/H_d .

To model the probability of bridge failure as a function of the flood intensity measure (IM), logistic regression is adopted. This approach is particularly suitable for binary response variables, herein defined as failure versus non-failure with respect to a specified damage threshold. The relationship between flood intensity and failure probability is formulated through a logistic function (Eqs. 2 and 3), which enables the estimation of exceedance probabilities across the full range of observed flood intensities. Through this data-driven formulation, the resulting fragility curves provide a transparent and statistically consistent representation of bridge vulnerability under flood loading conditions.

$$\text{Logit}(P) = \text{Ln}\left(\frac{P}{1-P}\right) \quad (2)$$

$$P = \frac{e^{(A+B.X)}}{1 + e^{(A+B.X)}} \quad (3)$$

where:

P is the probability of bridge failure, and X is the IM (H_w/H_d). A and B are the model coefficients determined using logistic regression.

Based on the observed bridge performance across multiple flood-intensity levels ($IM = H_w/H_d$), the failure probability at each level is obtained from the field data, and based on classification in Table 1, and its $\text{Logit}(P)$ is computed according to Eq. (2). Then, using *regression analysis*, the constant coefficients A (intercept) and B (slope) are calculated, and in Eq. (3), the only remaining variable is X , which is equal to IM, considering over a range of IM values (from very small to relatively large).

3 Case study

In 2019, a catastrophic flood in Poldokhtar, located in Lorestan Province, Iran, caused extensive damage to bridges. This study presents a detailed field investigation assessing the damage sustained by steel truss bridges during this flood. The findings are then used to generate empirical flood fragility curves for these structures.

The Kashkan River basin spans approximately 9,500 square kilometers, as illustrated in Fig. 3. Notably, in 2019, the river experienced a peak discharge of approximately 6,500

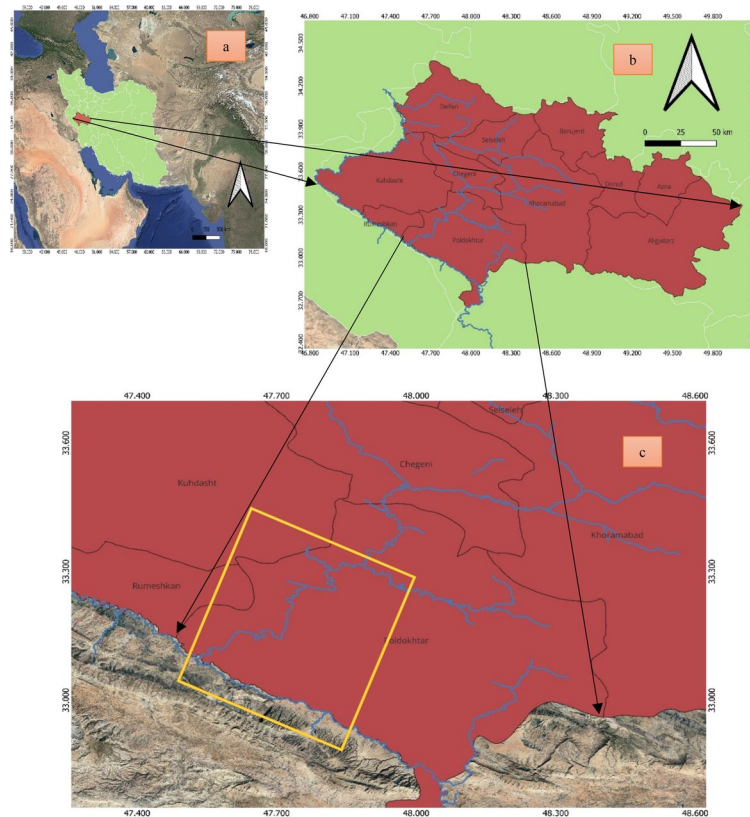


Fig. 3 Geographical framework of the Kashkan River Basin: **a** Iran with Lorestan Province highlighted, **b** the Kashkan River within Lorestan Province, and **c** the targeted study region

m^3/s , while its channel capacity was limited to only $2,400 \text{ m}^3/\text{s}$. This significant discrepancy underscores that the flood discharge far exceeded the river's capacity, leading to severe inundation and structural damage (Mirzaei 2019).

This study reports the performance of eight steel truss bridges (STBs) affected by extreme flooding and identifies common failure mechanisms. Figure 4 visualizes the studied steel truss bridges, while Table 3 shows the structural properties. As shown in Fig. 2, the deck truss is composed of multiple triangular units, each with a horizontal member length of 3 m and a vertical height of 3.6 m. All truss members are interconnected through pinned joints. The investigated bridges are as follows:

- STB1: Truss bridge in Doab village
- STB2: Truss bridge in Hayat-Algheyb village
- STB3: Truss bridge in Cham-Shahran village
- STB4: Truss bridge in Domroud-Afrineh village
- STB5: Truss bridge in Zivdar village
- STB6: Truss bridge in Kalat Zivdar village
- STB7: Truss bridge in Mazhin City
- STB8: Gavmishan truss bridge

4 Application of the methodology

The results of this study are presented through a structured three-step approach designed to capture both the empirical evidence and the analytical interpretation of flood impacts on bridges. First, field investigations were carried out to document the actual performance of the studied bridges during and after the flood, providing direct observational data on damage patterns and failure mechanisms. Second, statistical analyses were conducted to transform the field evidence into quantitative measures, including vulnerability and survival curves, which allowed for a probabilistic assessment of bridge performance under varying hazard levels. Finally, a kinematic approach was employed to further interpret the observed failure mechanisms by linking them to structural configurations and hydraulic interactions, thereby providing a mechanistic understanding of bridge responses to extreme flood conditions.

4.1 Field investigation

One of the key approaches to evaluating the vulnerability of various bridges to flooding is through post-flood field investigations to classify their performance. Truss bridges constitute about 57% of the bridges in this region. The behavior of eight bridges was scrutinized during and after the severe flood, revealing that only one bridge (STB4) maintained stability. Notably, out of the eight examined truss bridges, seven were destroyed (Fig. 5). For all bridges included in this study, the H_w/H_d ratio exceeded 1, except for STB2, which failed at an H_w/H_d value below 1. Detailed information about each bridge is provided below.

In bridges STB1, STB3, STB5, STB6, STB7, and STB8, the outflow was insufficient to handle the flood discharge due to debris damming on the upstream side of the bridges (debris damming phenomenon). This phenomenon caused water to accumulate on the upstream side of the structures, exerting additional pressure on their decks. Because of inadequate connection systems between the decks and the cap beams, piers, and abutments, the increased pressure from debris damming ultimately led to the collapse of these bridges (collapsed level).

In bridge STB1, additional pressure was exerted on the deck due to debris accumulation on the upstream side of the bridge, which reduced the outflow. Consequently, after the connection systems between the deck and the abutments failed, the deck slid and overturned (Fig. 5a). Figure 5b shows that the abutment was deformed and rotated due to flood-induced scouring, which led to the collapse of bridge STB2.

Upon examining the surface of abutments and cap beams of bridges STB3, STB5, STB6, STB7, and STB8, it is evident that there is no significant damage. This observation indicates that the decks in most of these bridges were placed on the substructures without any connection systems (Fig. 5f).

One of the critical factors influencing the severity of flood impacts on structures is the surrounding topography. In low-slope plain areas, floodwaters spread laterally across adjacent lands, dissipating energy and reducing the hydraulic pressure exerted on bridge components. Although Lorestan Province is predominantly mountainous, bridge STB4 is uniquely situated in a plain area.

Among all the truss bridges examined in this study, most experienced complete failure during the flood event; however, STB4 remained largely unaffected. This behavior is



a



b



c



d



e



f



g



h



i

Fig. 4 Photograph of bridge STB3 and map showing the geographical distribution of the eight investigated steel truss bridges. STB3 is shown as a representative example, since all bridges exhibit similar truss configurations and structural systems: **a** STB3, **b** STB1, **c** STB2, **d** STB3, **e** STB4, **f** STB5, **g** STB6, **h** STB7, and **i** STB8

Table 3 Properties of the studied bridges

Bridges	Identification	Type of superstructure	Type of substructure		
		Steel	Steel	RC	Masonry
The truss bridge in Doab village	STB1	*	*		
The truss bridge in Hayat-Algheyb village	STB2	*		*	
The truss bridge in Cham-Shahran village	STB3	*		*	
The truss bridge in Domroud-Afrineh village	STB4	*		*	
The truss bridge in Zivdar village	STB5	*			*
The truss bridge in Kalat Zivdar village	STB6	*			*
The Truss bridge in Mazhin city	STB7	*		*	
Gavmishan truss bridge	STB8	*		*	

The symbol * is used to express the type of substructure

likely influenced by its plain topographic setting, which may have reduced the hydraulic demand. In contrast, the strong connection system between the deck and substructure played a decisive role in ensuring the bridge's stability and preventing structural damage. A post-flood view of bridge STB4 is shown in Fig. 5d.

Figure 2 shows two critical connections in bridges. These connections can lead to bridge destruction under flooding if the connection systems are not properly designed. Seven of the eight steel truss bridges studied in this paper were destroyed. The cause of the destruction of six bridges was the improper connection of the deck to the substructure, which led to the deck sliding and overturning. Another bridge deck was overturned due to the scouring of the abutments. Notably, the occurrence of scour at the first flood-risk level and the ensuing failure show that bridge collapse can occur even at low flood severities ($IM < 0.75$) and is not restricted to high-intensity floods. Figure 6 shows a flowchart of the destroyed bridges (the cause of their damage) and stable bridges.

Among the main reasons for the destruction of bridges are the phenomena of debris damming and debris impact. If the water height is equal to or greater than the height of the deck, the accumulation of wood, trees, floating objects, etc., on the upstream side of the deck prevents parts of the water path. As a result of this process, the outflow water rate through the bridge is less than the water flow rate caused by the flood. For this reason, debris damming and debris impact occur. This phenomenon leads to water accumulation on the upstream side of the bridge. This process leads to extra pressure on the deck. This process is crucial for steel truss bridges, whose bracing members often trap debris, thereby intensifying flood-induced loads on such bridges. These phenomena can lead to the collapse of bridges if there is an improper connection between the deck and the substructure. Bridges STB1, STB3, STB5, STB6, STB7, and STB8 have been destroyed for the reason mentioned above. Figure 7 shows the location of the accumulation of wood and trees on the upstream side of the bridge deck.

In this study, one of the most critical causes of bridge failure is the inadequate strength of the connection system between the deck and the substructure. Figure 8 presents a schematic view of the cap beam surface after the deck sliding and overturning, showing that its surface remains undamaged. Figure 5f illustrates that, following the collapse of bridge STB6, no damage is observed on the cap beam surface. This indicates that no connection systems existed between this bridge's superstructure and the substructure.



Fig. 5 Post-flood conditions of the investigated steel truss bridges: **a** collapsed STB1, **b** STB2 collapsed due to abutment scour, **c** STB3 after the flood, **d** STB4 after the flood, **e** STB5 during flooding, **f** collapsed STB6, **g** STB7 during flooding, and **h** STB8 during flooding

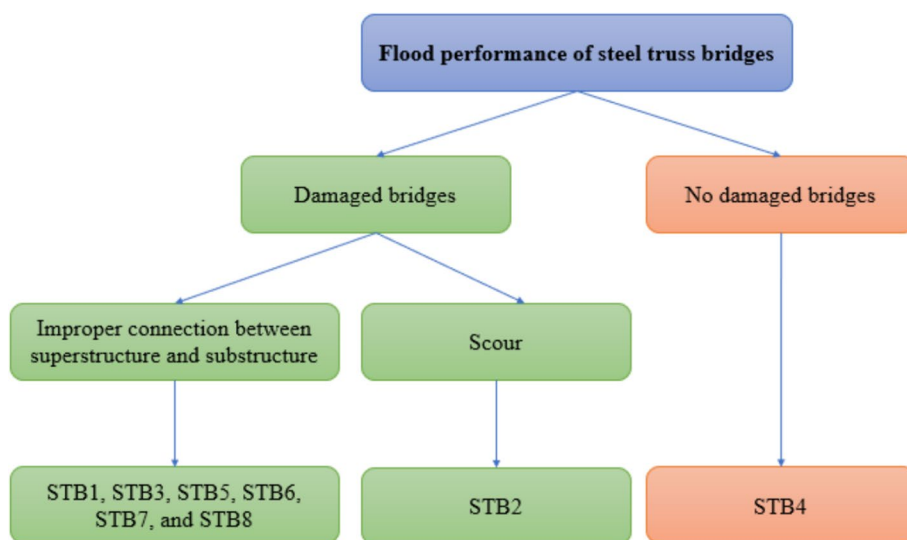


Fig. 6 Flowchart illustrating the classification of steel truss bridges as damaged or undamaged under flood conditions

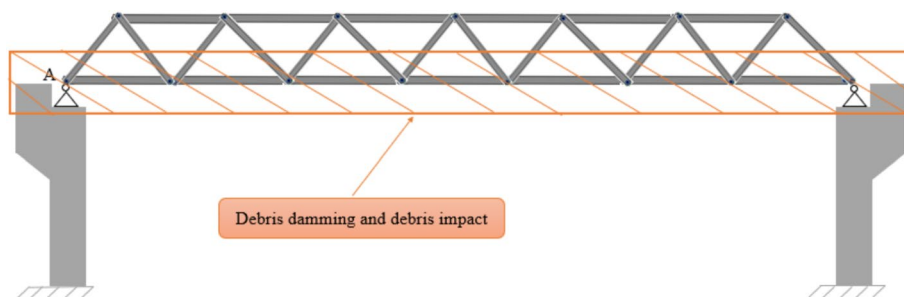


Fig. 7 The location of the observed accumulation of woody debris and floating objects

Figure 9 displays that the bridge STB4 has proper connections between the deck and the abutments.

4.2 Statistical analysis

As shown in Fig. 10, 12.5% of the bridge failures are attributed to scouring, at hazard level I. At hazard level II. Only 12.5% of the studied bridges remained stable, and 75% of the studied bridges failed due to deck sliding and overturning at hazard level III, as the water level exceeded the bridge deck.

The empirical assessment of flood-induced vulnerability using the H_w/H_d index shows that, at hazard level I, bridge STB2 overturned due to scouring effects on its abutment. At hazard level II, no additional bridge failures were observed. At hazard level III, six bridges (STB1, STB3, STB5, STB6, STB7, and STB8) collapsed due to deck sliding and overturning caused by improper connections between the superstructure and substructure, instability of the bridges, debris damming, and excessive hydrodynamic forces. Only STB4 remained stable, demonstrating resilience under extreme flood conditions. In this context, the percentage of failed bridges at different hazard levels is analyzed (Fig. 11). The results from Fig. 8 indicate that when the

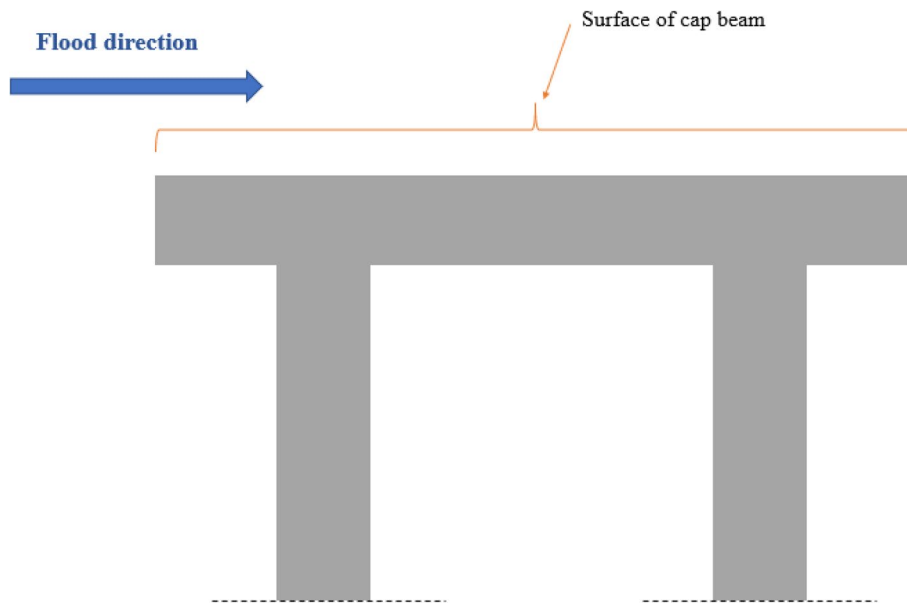


Fig. 8 The schematic representation of the cap beam in the most studied bridge after the collapse



Fig. 9 Connection configuration between the superstructure and substructure in bridge STB4

H_w/H_d parameter exceeds 1 (third hazard level), the rate of bridge failure increases significantly.

Figure 12 presents the Kaplan–Meier survival curve for bridges under varying flood intensity ratios (H_w/H_d). When the H_w/H_d index is equal to 0.75, one bridge failure is recorded, reducing the survival probability to 0.875. No further failures occur when H_w/H_d index is equal to 1.0, and the survival probability remains unchanged. However, when H_w/H_d reaches 1.2, six additional bridges fail, leading to a sharp decline in survival probability to nearly 0.125. This steep drop indicates that most failures occur

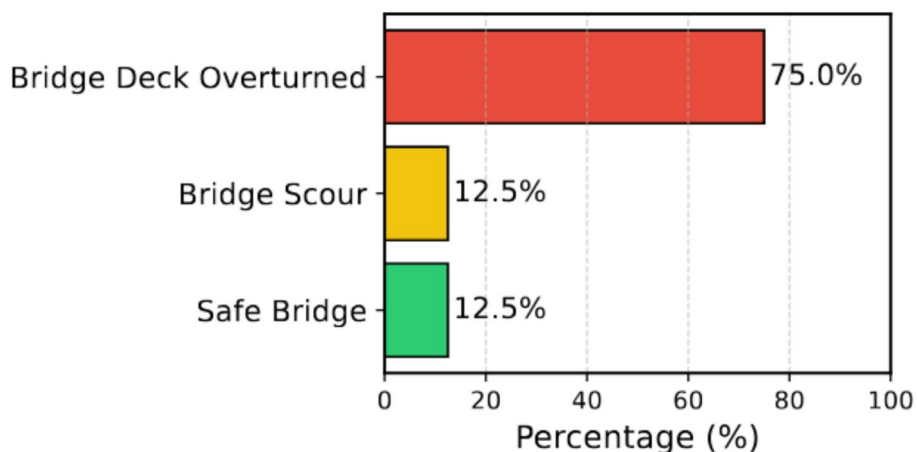


Fig. 10 Distribution of flood-induced damage states in investigated bridges

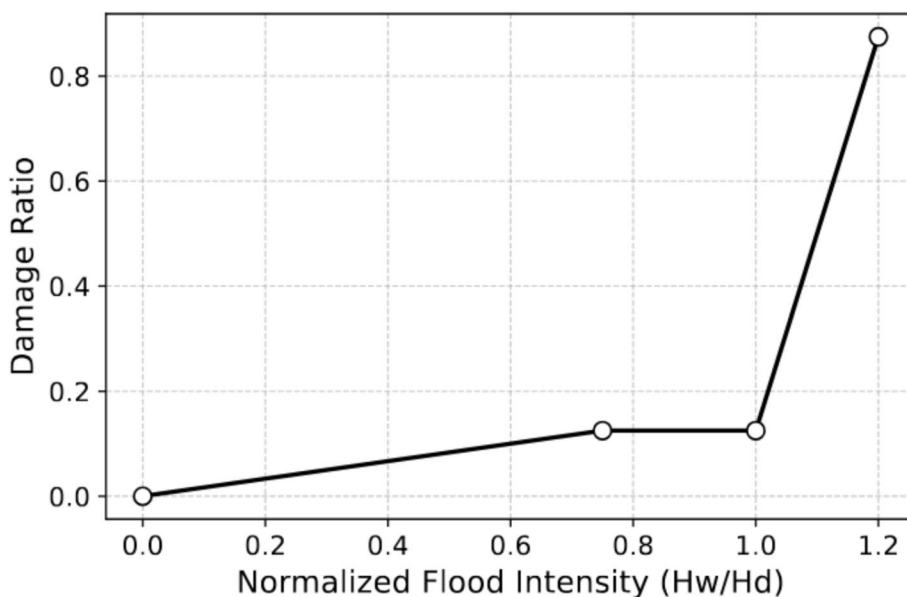


Fig. 11 Empirical flood vulnerability curve depicting the relationship between parameter H_w/H_d and the damage ratio of bridges

once the flood intensity surpasses a critical threshold, emphasizing the importance of considering the H_w/H_d criterion in the design of river-crossing bridges to ensure reliability against severe flooding.

As presented in Fig. 13, the empirical fragility curve illustrates the increasing probability of failure of steel truss bridges with rising values of the intensity measure ($IM = H_w/H_d$). For example, when H_w/H_d is 0.1, the probability of bridge failure is as low as 0.034%. When the H_w/H_d index is equal to 1.5 (corresponding to water depths ranging from 0.01 to 1.8 m), the failure probability sharply increases to 97.4%. This probabilistic representation provides valuable insights into the vulnerability of steel truss bridges under flood conditions and serves as a robust tool for risk assessment and flood

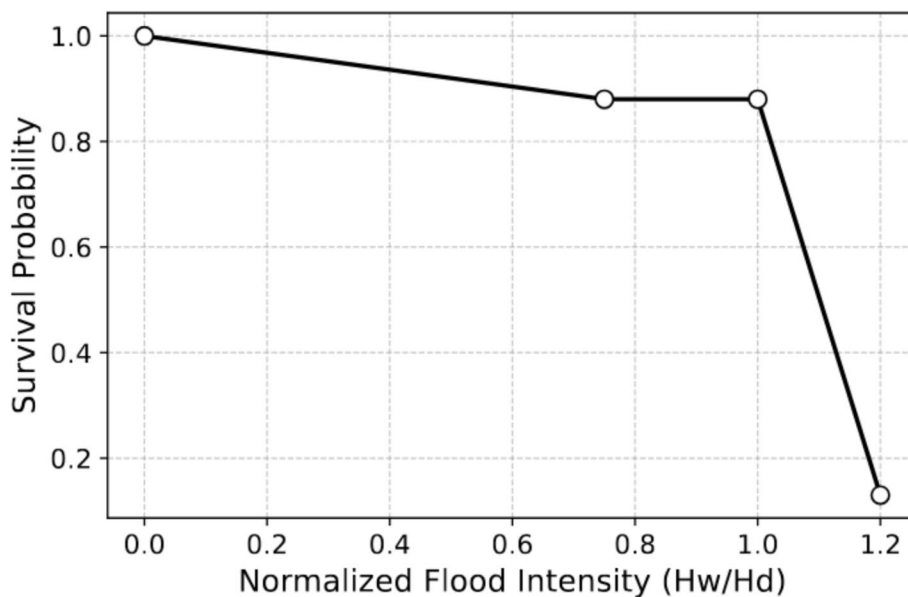


Fig. 12 Kaplan–Meier survival curve illustrating bridge reliability under varying flood intensity ratios (Hw/Hd)

management planning. The developed fragility curve represents a practical instrument for assessing flood-related risks and planning management strategies, enabling engineers, stakeholders, and policymakers to gain deeper insights into the susceptibility of steel truss bridges under diverse hydraulic conditions.

5 Conclusion

This study presents a methodology for developing empirical flood fragility curves for steel truss bridges. Based on post-flood field surveys, expert damage classification, and engineering judgment, the proposed approach captures observed failure mechanisms and explains bridge collapses even under relatively low hazard levels. The resulting fragility curves offer a transparent and data-driven framework for emergency response planning and retrofit prioritization, while also acknowledging existing limitations and identifying directions for future improvement. The main conclusions are summarized below:

The destruction of approximately 87.5% of the steel truss bridges in this region highlights a significant disruption in the road communication network, with 7 out of 8 studied bridges being destroyed.

The collapsed bridges were located in mountainous areas, while the sole, safe steel truss bridge was in a plain region. Flood depth is a critical factor in determining bridge damage, and it is more severe in mountainous areas than in plains.

Maintaining an adequate water-to-deck elevation ratio during high-probability flood events is critical; the deck must remain far from the water surface to prevent debris damming effect, hydrodynamic uplift, extra loads, and ensuing instability.

Bridges STB1, STB3, STB5, STB6, STB7, and STB8 experienced an IM greater than one, resulting in the collapse of their decks.

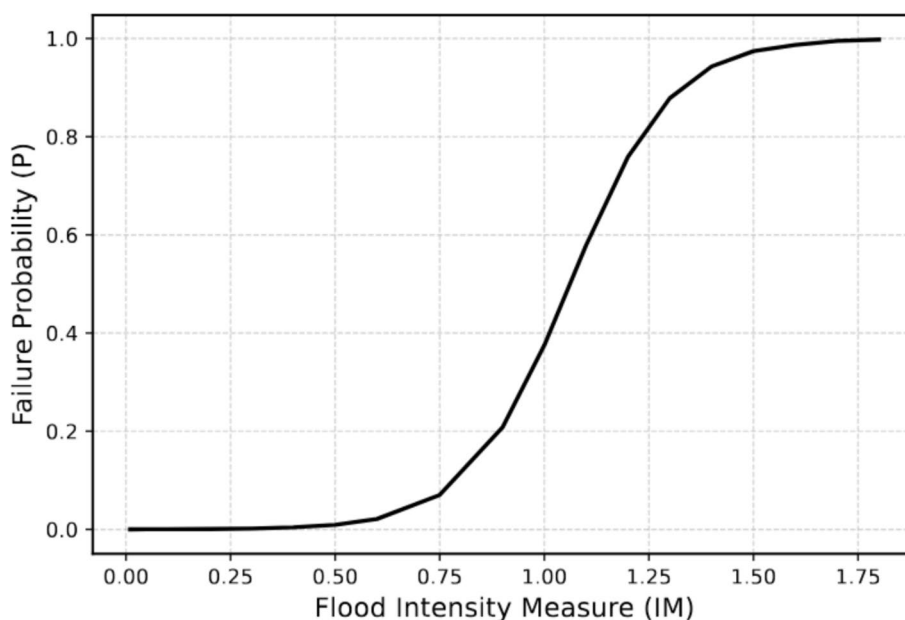


Fig. 13 Empirical fragility curve illustrating the probability of failure of steel truss bridges as a function of intensity measure

Bridge STB2 collapsed before the water level reached the deck height due to abutment scouring and rotation.

Although Bridge STB4 experienced an IM greater than one, it remained stable under flood conditions for two main reasons. First, it is located in a plain area, where floodwater can spread laterally, leading to a dissipation of hydraulic energy compared to mountainous settings. Second, the bridge deck is adequately connected to the abutments, which enhances its stability during the flood event.

The results of the survival and fragility curves indicate that when the water level increases during a flood, the extent of bridge damage also rises. Specifically, when the floodwater height (H_w) is greater than the deck height ($H_w/H_d \geq 1$), the probability of bridge failure significantly increases. These findings emphasize the importance of considering this factor in designing flood-resistant steel truss bridges to prevent widespread structural damage.

While most analytical methodologies presuppose a monotonic and well-defined correlation between flood intensity and bridge damage, the empirical evidence gathered in this study reveals noticeable deviations from such idealized patterns. This result, often overlooked or simplified in conventional hydraulic and numerical models, highlights the limitations of purely theoretical approaches. Consequently, the empirical fragility curves developed herein are firmly rooted in observed field performance, providing a data-driven representation that explicitly incorporates real-world irregularities into bridge vulnerability assessment under flood hazards.

Field evidence indicates that deck inundation ($H_w/H_d \geq 1$) is the primary mechanism leading to bridge failure. Therefore, in the design of new bridges, the deck elevation must be sufficiently higher than extreme flood levels, particularly in mountainous regions.

Inadequate connection systems between the deck and substructure were among the most important causes of deck uplift and rotation. Strengthening the connections and increasing the anchorage capacity against uplift forces can significantly reduce the likelihood of failure.

Scouring was one of the key mechanisms of structural damage. Effective countermeasures include the use of deeper foundations such as piles and micropiles, appropriate bed protection measures—especially around piers and abutments—and installing scour monitoring systems to obtain reliable estimates of scour progression.

Accurate assessment of the ratio between the natural channel discharge capacity and the peak flood discharge, as well as the ratio between the bridge outflow capacity and the peak flood discharge, is essential in the design of new bridges and in the retrofit planning of existing ones.

The accumulation of debris, tree trunks, and vegetation—and the formation of debris dams—plays a significant role in increasing hydraulic forces and pressures on the deck. Therefore, implementing periodic debris management and upstream clearing strategies can substantially mitigate this phenomenon.

Enhancing the flood resilience of bridges requires the deployment of structural and hydraulic health monitoring systems, as well as flood early-warning systems.

Loose soils (land) surrounding the river are susceptible to erosion and scour during floods, and large volumes of sediment may enter the flow, increasing sediment load, altering flow patterns, and intensifying hydrodynamic forces on bridges. Therefore, stabilizing vulnerable soils along the riverbanks is of high importance.

In summary, the proposed framework (relying solely on the intensity measure $IM = H_w/H_d$ under data-scarce conditions) provides an effective tool for risk assessment of truss bridges. Its main advantages are: (i) it explicitly incorporates flood-to-deck elevation ratio, a highly influential descriptor of flood severity; and (ii) for existing steel truss bridges, it can be a reasonable estimate of failure probability that can serve as a practical basis for retrofit prioritization and is even an effective factor in bridge design. Nevertheless, although IM is a suitable index for comparing diverse conditions, it does not capture all hydraulic factors; in this study, the focus is restricted to the water-level-to-deck-elevation ratio. With more comprehensive data, the index should be extended to a multi-parameter measure that augments IM with the ratio of flood discharge to the natural channel capacity, the ratio of flood discharge to the bridge's outflow capacity, the effects of flow velocity and flood duration, and the prevalence of floating debris and vegetation along the flow path (which contribute to debris damming). Accordingly, the present results should be viewed as a data-driven basis for initial decision-making. In subsequent cycles, this IM is improved toward more precise predictions by incorporating additional hydraulic parameters.

Acknowledgements

The authors gratefully acknowledge FABRE (Research consortium for the evaluation and monitoring of bridges, viaducts, and other structures). Any opinions expressed in this paper do not necessarily reflect the views of the funders.

Authors' contributions

Saman Mansouri: Writing—review & editing, Writing—original draft, Methodology, Investigation, Conceptualization. Ilaria Venanzi: Writing—review & editing, Supervision, Methodology, Conceptualization. Filippo Ubertini: Writing—review & editing, Supervision, Methodology, Conceptualization. Chiara Biscarini: Writing—review & editing, Supervision, Methodology, Conceptualization.

Funding

This study was supported by FABRE (www.consorziofabre.it/en) within the activities of the FABRE-ANAS 2021–2026 research program.

Data availability

All data generated or analyzed during this study are included in this published article.

Declarations

Competing interests

The authors declare that they have no competing interests.

Received: 29 October 2025 Revised: 23 December 2025 Accepted: 4 January 2026

Published online: 20 April 2026

References

- Ahamed T, Duan JG, Jo H (2021) Flood-fragility analysis of in-stream bridges—consideration of flow hydraulics, geotechnical uncertainties, and variable scour depth. *Struct Infrastruct Eng* 17(11):1494–1507. <https://doi.org/10.1080/15732479.2020.1815226>
- Allen E, Costello SB, Henning TFP, Chamorro A, Echaveguren T (2023) Integration of resilience and risk to natural hazards into transportation asset management of road networks: a systematic review. *Struct Infrastruct Eng* 21(5):755–773. <https://doi.org/10.1080/15732479.2023.2238281>
- Argyroudis SA, Mitoulis SA (2021) Vulnerability of bridges to individual and multiple hazards- floods and earthquakes. *Reliab Eng Syst Saf* 210. <https://doi.org/10.1016/j.res.2021.107564>
- Arora RK, Banerjee S (2023) Reliability-based approach for fragility assessment of bridges under floods. *Struct Eng Mech* 88(4):311–322. <https://doi.org/10.12989/sem.2023.88.4.311>
- Ataei N, Padgett JE (2013) Limit state capacities for global performance assessment of bridges exposed to hurricane surge and wave. *Struct Saf* 41:73–81. <https://doi.org/10.1016/j.strusafe.2012.10.005>
- Barbera RM, Lanzarote BS, Escrig T, Cabrera-Fausto I (2024) Characterization of damages in buildings after floods in Vega Baja County (Spain) in 2019. The case study of Almoradí municipality. *Case Stud Constr Mater* 20:e03004. <https://doi.org/10.1016/j.cscm.2024.e03004>
- Burghardt L, Klopries EM, Schüttrumpf H (2025) Structural damage, clogging, collapsing: analysis of the bridge damage at the rivers Ahr, Inde and Vicht caused by the flood of 2021. *J Flood Risk Manag* 18(1). <https://doi.org/10.1111/jfr3.13001>
- Cartiaux FB, Legoll F, Libal A, Reygnier J (2024) Survival probability of structures under fatigue: a data-based approach. *Probabilistic Eng Mech* 77:103657. <https://doi.org/10.1016/j.probengmech.2024.103657>
- Chung HCP, Adeyeye K (2018) Structural flood damage and the efficacy of property-level flood protection. *Int J Build Pathol Adapt* 36(5):471–499. <https://doi.org/10.1108/IJBPA-09-2017-0040>
- Cicco PND, Paris E, Solari L, Ruiz-Villanueva V (2020) Bridge pier shape influence on wood accumulation: outcomes from flume experiments and numerical modeling. *J Flood Risk Manag* 13. <https://doi.org/10.1111/jfr3.12599>
- De Risi R, Jalayer F, De Paola F, Carozza S, Yonas N, Giugni M, Gasparini P (2020) From flood risk mapping toward reducing vulnerability: the case of Addis Ababa. *Nat Hazards* 100:387–415. <https://doi.org/10.1007/s11069-019-03817-8>
- Drdáček MF (2010) Flood damage to historic buildings and structures. *J Perform Constr Facil* 24(5):439–445. [https://doi.org/10.1061/\(ASCE\)CF.1943-5509.0000065](https://doi.org/10.1061/(ASCE)CF.1943-5509.0000065)
- Fang J, Ishida T, Yamazaki T (2018) Quantitative evaluation of risk factors affecting the deterioration of RC deck slab components in East Japan and Tokyo regions using survival analysis. *Appl Sci* 8(9):1470. <https://doi.org/10.3390/app8091470>
- Greco F, Lonetti P (2022) Vulnerability analysis of structural systems under extreme flood events. *J Mar Sci Eng* 10(8). <https://doi.org/10.3390/jmse10081121>
- Guikema S, Gardoni P (2009) Reliability estimation for networks of reinforced concrete bridges. *J Infrastruct Syst* 15(2). [https://doi.org/10.1061/\(ASCE\)1076-0342\(2009\)15:2\(61\)](https://doi.org/10.1061/(ASCE)1076-0342(2009)15:2(61))
- Habeeb B, Bastidas-Arteaga E (2023) Assessment of the impact of climate change and flooding on bridges and surrounding area. *Front Built Environ* 9:1268304. <https://doi.org/10.3389/fbuil.2023.1268304>
- Han Y, Chun Q, Gao X (2023) Flood-induced forces and collapse mechanism of historical multi-span masonry arch bridges: the Putang bridge case. *Eng Fail Anal* 153:107564. <https://doi.org/10.1016/j.engfailanal.2023.107564>
- Hasanpour A, Istrati D, Buckle I (2022) Multi-physics modeling of tsunami debris impact on bridge decks. In: 3rd International Conference on Natural Hazards & Infrastructure, Athens, Greece
- Jonkman SN, Vrijling JK, Vrouwenvelder ACWM (2008) Methods for the estimation of loss of life due to floods: a literature review and a proposal for a new method. *Nat Hazards* 46:353–389. <https://doi.org/10.1007/s11069-008-9227-5>
- Karriqi T, Matos JC, Dang NS, Xia Y (2024) Bridge assessment under earthquake and flood-induced scour. *Appl Sci* 14:5174. <https://doi.org/10.3390/app14125174>
- Kelesoglu MK, Temur R, Gülbaz S, Apaydin NM, Kazezyılmaz-Alhan CM, Bozbey I (2023) Site assessment and evaluation of the structural damages after the flood disaster in the Western Black Sea Basin on August 11. *Nat Hazards* 116:587–618. <https://doi.org/10.1007/s11069-022-05690-4>

- Kerenyi K, Sofu T, Guo J (2009) Hydrodynamic forces on inundated bridge decks. Research, Development, and Technology, Turner-Fairbank Highway Research Center, Federal Highway Administration (FHWA), Report No. FHWA-HRT-09-028, 2009
- Kim H, Sim SH, Lee J, Lee YJ, Kim JM (2017) Flood fragility analysis for bridges with multiple failure modes. *Adv Mech Eng* 9(3):1–11. <https://doi.org/10.1177/1687814017696415>
- Komolafe AA, Ogundare AS, Olorunfemi IE, Oguntunde PG (2024) Flood damage models and flood damage factors in a data-scarce river basin, Nigeria. *Environ Hazards* 1–28. <https://doi.org/10.1080/17477891.2024.2394206>
- Kosic M, Anžlin A, Bau V (2023) Flood vulnerability study of a roadway bridge subjected to hydrodynamic actions, local scour and wood debris accumulation. *Water* 15:129. <https://doi.org/10.3390/w15010129>
- Lamb R, Garside P, Pant R, Hall JW (2019) A probabilistic model of the economic risk to Britain's railway network from bridge scour during floods. *J Risk Anal* 39(11). <https://doi.org/10.1111/risa.13370>
- Lee GC, Mohan SB, Huang C, Fard BN (2013) A study of U.S. bridge failure (1989–2012). Technical report MCEER-13-0008, 2013
- Mansouri S (2020) The investigation of the effects of vertical earthquake component on seismic response of skewed reinforced concrete bridges. *Int J Bridge Eng* 8(1):35–52
- Mansouri S (2021) The investigation of the effect of using energy dissipation equipment in seismic retrofitting an existing highway RC bridge subjected to far-fault earthquakes. *Int J Bridge Eng* 9(3):51–84
- Mansouri S, Pouraminian M (2022) The investigation of the damages of bridges subjected to the 2020 flood in Poldokhtar (Iran). *Int J Bridge Eng* 10(1):43–77
- Mansouri S, Kontoni DPN, Pouraminian M (2022) The effects of the duration, intensity, and magnitude of far-fault earthquakes on the seismic response of RC bridges retrofitted with seismic bearings. *Adv Bridge Eng* 3:19. <https://doi.org/10.1186/s43251-022-00069-8>
- Mansouri S, Noroozinejad Farsangi E (2024) Adequacy of equivalent static analysis method employing Caltrans, AASHTO, and ATC-32 provisions in response estimation of vibration-controlled bridges. *ASCE's J Struct Design Constr Pract* 29(1). <https://doi.org/10.1061/PPSCFX.SCENG-1340>
- Mansouri S, Pouraminian M, Noroozinejad Farsangi E (2024) Bridges damaged during the 2019 flood in Poldokhtar toward flood hazard resilient bridges. In: Proceedings of the Institution of Civil Engineers: Bridge Engineering. <https://doi.org/10.1680/jbren.22.00050>
- Mansouri S, Noroozinejad Farsangi E, Siahpolo N, Moghadam AS, Karimipour A, Noori M (2025) Effects of river shapes on structural damages to buildings in flood-prone regions. *ASCE's J Struct Design Constr Pract* 30(3). <https://doi.org/10.1061/JSDCCC.SCENG-1717>
- Marvi MT (2020) A review of flood damage analysis for a building structure and contents. *Nat Hazards* 102:967–995. <https://doi.org/10.1007/s11069-020-03941-w>
- Mirzaei R (2019) A comprehensive report for the 2019 flood in Poldokhtar. Regional Water Company of Lorestan Province, Lorestan, Iran. (In Farsi)
- Mitoulis SA, Domaneschi M, Cimellaro GP, Casas JR (2022) Bridge and transport network resilience—a perspective. *Proc Inst Civ Eng Bridge Eng* 175(3):138–149. <https://doi.org/10.1680/jbren.21.00055>
- Mitoulis SA, Argyroudis SA, Loli M, Imam B (2021) Restoration models for quantifying flood resilience of bridges. *Eng Struct* 238. <https://doi.org/10.1016/j.engstruct.2021.112180>
- Okamoto T, Takebayashi H, Sanjou M, Suzuki R, Toda K (2020) Log jam formation at bridges and the effect on floodplain flow: a flume experiment. *J Flood Risk Manag* 13. <https://doi.org/10.1111/jfr3.12562>
- Padgett JE, Spiller A, Arnold C (2012) Statistical analysis of coastal bridge vulnerability based on empirical evidence from hurricane Katrina. *Struct Infrastruct Eng* 8:595–605. <https://doi.org/10.1080/15732470902855343>
- Panici D, de Almeida GAM (2020) Influence of pier geometry and debris characteristics on wood debris accumulations at bridge piers. *J Hydraul Eng* 146(6). [https://doi.org/10.1061/\(ASCE\)HY.1943-7900.0001757](https://doi.org/10.1061/(ASCE)HY.1943-7900.0001757)
- Paulik R, Wild A, Zorn C, Wotherspoon L (2022) Residential building flood damage: insights on processes and implications for risk assessments. *J Flood Risk Manag* 15(4). <https://doi.org/10.1111/jfr3.12832>
- Pistrika A, Tsakiris G (2007) Flood risk assessment: a methodological framework. In: Water resources management: new approaches and technologies, European Water Resources Association, Chania, Crete, Greece
- Pucci A, Eickmeier D, Sousa HS, Giresini L, Matos JC, Holst R (2023) Fragility analysis based on damaged bridges during the 2021 flood in Germany. *Appl Sci* 13:10454. <https://doi.org/10.3390/app131810454>
- Rezvani SMHS, Silva MJF, de Almeida NM (2024) Urban resilience index for critical infrastructure: a scenario-based approach to disaster risk reduction in road networks. *Sustainability* 16:4143. <https://doi.org/10.3390/su16104143>
- Scawthorn C, Blais N, Seligson H, Tate E et al (2006a) HAZUS-MH flood loss estimation methodology. I: Overview and flood hazard characterization. *Nat Hazards Rev* 7(2). [https://doi.org/10.1061/\(ASCE\)1527-6988\(2006\)7:2\(60\)](https://doi.org/10.1061/(ASCE)1527-6988(2006)7:2(60))
- Scawthorn C, Flores P, Blais N et al (2006b) HAZUS-MH flood loss estimation methodology. II. damage and loss assessment. *Nat Hazards Rev* 7(2):72. [https://doi.org/10.1061/\(ASCE\)1527-6988\(2006\)7:2\(72\)](https://doi.org/10.1061/(ASCE)1527-6988(2006)7:2(72))
- Torres MA, Jaimes MA, Reinoso E, Ordaz M (2014) Event-based approach for probabilistic flood risk assessment. *Int J River Basin Manage* 12(4). <https://doi.org/10.1080/15715124.2013.847844>
- Wang T, Liu Y, Li Q, Du P, Zheng X, Gao Q (2023) State-of-the-art review of the resilience of urban bridge networks. *Sustainability* 15(2):989. <https://doi.org/10.3390/su15020989>
- Wang W, Zhou K, Jing H, Zuo J, Li P, Li Z (2019) Effects of bridge piers on flood hazards: a case study on the Jialing River in China. *J Water* 11(6). <https://doi.org/10.3390/w11061181>
- Wettach-Glosser J, Unnikrishnan A, Schumacher T (2020) Survival analysis of concrete highway bridge decks in Oregon utilizing LASSO and stepwise-variable selection. *J Bridge Eng*. [https://doi.org/10.1061/\(ASCE\)BE.1943-5592.0001606](https://doi.org/10.1061/(ASCE)BE.1943-5592.0001606)
- Xia J, Teo FY, Falconer RA, Chen Q, Deng S (2018) Hydrodynamic experiments on the impacts of vehicle blockages at bridges. *J Flood Risk Manag* 11. <https://doi.org/10.1111/jfr3.12228>
- Xiao S, Li N, Guo X (2021) Analysis of flood impacts on masonry structures and mitigation measures. *J Flood Risk Manag*. <https://doi.org/10.1111/jfr3.12743>
- Xiaofei M, Junxiang S, Jiahua Z, Wenzhe W (2024) Analysis of flood resistance of masonry arch bridges combining numerical simulation and probabilistic analysis. *Int J Archit Heritage*. <https://doi.org/10.1080/15583058.2024.2408693>

Yilmaz T, Banerjee S (2018) Impact spectrum of flood hazard on seismic vulnerability of bridges. *Struct Eng Mech* 66(4):515–529. <https://doi.org/10.12989/sem.2018.66.4.515>

Publisher's Note

Springer Nature remains neutral with regard to jurisdictional claims in published maps and institutional affiliations.